GEOCHRONOMETRIA 48 (2021): 284–293
DOI 10.2478/geochr-2020-0012

Available online at
https://content.sciendo.com/view/journals/geochr/geochr-overview.xml

Conference Proceedings of the 5th Asia Pacific Luminescence and Electron Spin Resonance Dating Conference
October 15th-17th, 2018, Beijing, China

Guest Editor: Grzegorz Adamiec

HOLOCENE OSL CHRONOLOGY OF FLU-LACUSTRINE SEDIMENTS IN YANGTZE RIVER BASIN, WUHAN AREA, CHINA

CHUANYI WEI[1], HUASONG ZHANG[1], CHANG'AN LI[1, 2], YUFEN ZHANG[3], YAWEI LI[1], MINGMING JIA[1], GUOQING LI[1] and YONGHUI LENG[1]

[1]*School of Earth Sciences, China University of Geosciences, Wuhan 430074, China*
[2]*Hubei Key Laboratory of Critical Zone Evolution, China University of Geosciences, Wuhan 430074, China*
[3]*Institute of Geophysics and Geomatics, China University of Geosciences, Wuhan 430074, China*

Received 20 December 2018 Accepted 7 November 2019

Abstract: Wuhan area located middle Yangtze River Basin, is dominated by East Asian Monsoon. Widely developed Holocene flu-lacustrine sediments are ideal materials for the reconstruction of paleoclimate change and geo-environment evolution, for which the chronology is a key issue. In this study, 20 luminescence dating samples were collected from a flu-lacustrine sequence and the reliability of the quartz OSL dating to these samples were checked by using luminescence characteristics of dose recovery test and thermos transfer test. Our results indicate that different grain size fraction of 4~11 μm, 38~63 μm, and 90~125 μm were well-bleached before burial. Dating results show that all these ages range from 0.8 ± 0.1 to 7. 9 ± 0.7 ka between 4.25 and 38.55 m, and most of them follow the stratigraphic sequence and other climatic recorder within the normal range of error. Disordered OSL ages may be caused by complicated transport-deposit processes. As a consequence, OSL dating method of SAR-SGC protocol could provide a significant chronology for Holocene flu-lacustrine sediment in large river depo-system.

Keywords: Luminescence dating, quartz, flu-lacustrine sediment, Holocene, Wuhan area, the Yangtze River Basin.

1. INTRODUCTION

The Yangtze River, which is dominated by the strongest monsoon climate conditions (**Fig. 1a**), delivers large volumes of water, chemicals and sediment from its headwater regions and tributaries to middle-lower reaches and East China Sea, not only significantly influencing sedimentary system evolution in its drainage basin, but also greatly affect ecological environment and human activities (Wang *et al.*, 2017; Zhang *et al.*, 2015). In addition, over 400 million people – 6.6% of the world's population – lived in the Yangtze River Basin with a catchment of more than 1.8×10^6 km^2 (Sun *et al.*, 2016). Particularly, Wuhan area, as the biggest city located middle Yangtze River Basin, has hundreds of lakes and Yangtze River mainstream drained here, is of great significance to understand paleoclimate change and paleo-environment evolution.

Corresponding author: C. Li
e-mail: chanli@cug.edu.cn

ISSN 1897-1695 (online), 1733-8387 (print)

The Holocene is the current geological epoch, and it has seen the growth and impacts of the human species worldwide, including all its written history, development of major civilisations, and overall significant transition toward urban living in the present. During this period, changes of the natural environment and climate play a key role in the development and progress of human civilisation. Thus, effects of Holocene climate change and geo-environmental evolution on human have been received more and more attention (Zhou *et al.*, 2005; Prokopenko *et al.*, 2007; Wallinga, 2010; Ashley *et al.*, 2011; Briner *et al.*, 2016; Marks *et al.*, 2017; Guo *et al.*, 2018). Recently, a high-resolution and accurate geochronological framework of flu-lacustrine sediments, which are important records of paleo-environment and paleoclimate, allows us to understand these phenomena better.

Radiocarbon dating is widely used for lacustrine sediment chronology determination (Long *et al.*, 2011). However, ^{14}C dating of such sediments could be problematic because they often suffer from contamination from sources of 'old carbon' (hard water reservoir effect) (Liu *et al.*, 2009) and the reservoir effect (Wang *et al.*, 2007; Queiroz *et al.*, 2018; Xu *et al.*, 2018). In addition, lack of continuous and suitable dating materials also makes it a challenging work to obtain accurate chronologies of fluvial-lacustrine sediment by ^{14}C dating. In nearly two decades, optically stimulated luminescence (OSL) dating had been widely applied to dating lake sediments in order to improve the ^{14}C dating problems (English *et al.*, 2001; Berger and Doran, 2001; Olley *et al.*, 2004; Cupper, 2008; Madsen *et al.*, 2008; Fan *et al.*, 2010; Liu *et al.*, 2009; Shen *et al.*, 2015; Ozcelik, 2016; Hu *et al.*, 2017; Lehmann *et al.*, 2017; Zhao *et al.*, 2015; Ideker *et al.*, 2017; May *et al.*, 2018; Harning *et al.*, 2018).

In this study, we collected 20 samples from the 45 m long Holocene core HH-2017 (30°37'59.20" N, 114°17'21.43" E) in middle Yangtze River Basin, Wuhan area, China for OSL dating, in order to establish high-resolution chronology of flu-lacustrine sediment for better understanding regional paleo-climatic changes and geo-environmental evolution.

2. STUDYING AREA, CORING AND SAMPLING

Wuhan area is located eastern Jianghan Basin, middle Yangtze River Basin, **Fig. 1b**. This region is dominated by the summer monsoon from June to September, which brings most of the moisture for the whole year. In winter, cold and wet continental air mass prevailed in the area. The mean annual temperature of Wuhan is between 13.4°C and 18.5°C while the annual precipitation is about 1300 mm (http://www.hbqx.gov.cn/news.action?id=6530). Subtropical monsoon climate and downland mound make Wuhan area composed of high-density river drainages and numerous lake systems, **Fig. 1c**. The water covers 1/4 of the land area with more than 2117 km^2, including 471 km^2 river channel and 868 km^2 lacustrine coverage. As a consequence, Wuhan area widely developed 30~40 m Holocene flu-lacustrine deposits.

Considering of regional geomorphological/geological setting and human activities, in autumn field work of 2017, a 45 m long core (114°17'21.43" E, 30°37'59.20" N, 26 m above sea level) is extracted from the left bank floodplain, which is 3 km far away from the Yangtze River, **Fig. 1c**. From bottom upwards the core, the deposits grain size become finer and finer from gravel to silt. It shows a typical flu-lacustrine depo-system and can be

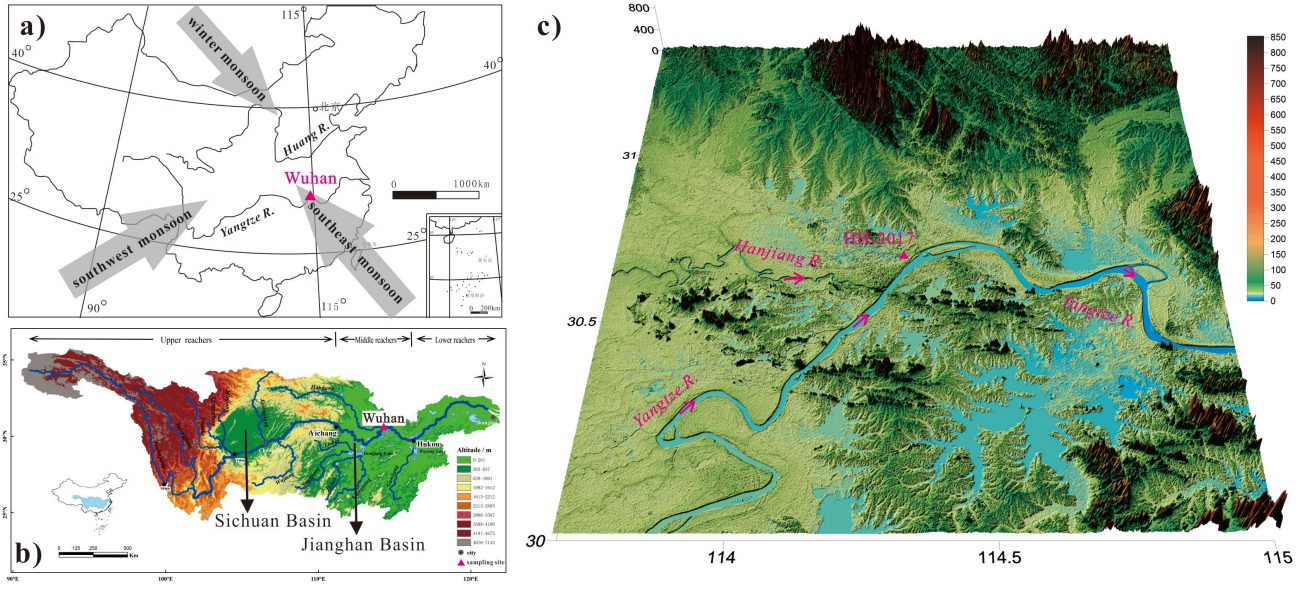

Fig. 1. *Location of core HH-2017. a) and b) Wuhan area located in middle Yangtze River Basin is dominated by East Asian monsoon; c) map showing hundreds of lakes and rivers developed in Wuhan area; core HH-2017 was drilled in left bank of Yangtze River.*

divided into 11 layers according to variations in colour, texture and lithology, **Fig. 2**. Before 4.25 m, it is artificial backfill soil layer while no suitable materials for OSL dating after 38.55 m, thus, 20 samples were collected for OSL dating from 4.25 m to 38.55 m. In practical sampling work, we cannot collect samples with an equal distance because of the unconsolidated formation and partly low core recovery rate, detailed information seen in **Fig. 2** and **Table 1**. To avoid exposure to light, each columnar OSL dating sample were put into an algam-made container just after drilling done.

3. METHODS

Quartz extraction and measurement techniques

Quartz extraction and OSL measurement were conducted in OSL Dating Laboratory, China University of Geosciences (Wuhan). In the laboratory, outermost sediment of each core OSL dating sample was scraped to avoid potential contamination inherited from drilling and sampling. Then, we scraped more outer possible light-exposed materials used for dose rate and water content measurement. The left non-light-exposed materials in the middle part of the container were prepared for quartz extraction.

The non-light-exposed materials were treated firstly with 30% H_2O_2 and 10% HCl to remove organic materials and carbonates, respectively. For different grain size sedimentary layer, the 4~11 μm, 38~63 μm and 90~125 μm fractions were separated by wet sieving. Especially, the fine silt (4–11 μm) was obtained using sedimentation procedures based on Stokes' Law (Lu *et al.*, 2007). After that, on the one hand, the 4~11 μm and the 38~63 μm fractions were treated with H_2SiF_6 (38%) for about 2 weeks to corrode feldspars, followed by 10% HCl to remove fluoride precipitates. On the other hand, sodium polytungstate was used to separate the 90~125 μm materials of the density ranging between 2.62 and 2.70 g/cm^{-3}, and a density of 2.75 g/cm^{-3} heavy liquid was used to remove heavy minerals. Then the materials were treated with 40% HF for 40 min to remove feldspars and the part of grains affected by alpha particles and were treated with fluorosilicic acid (38%) for about 5 days and followed by 10% HCl for 5 hours. Magnetic minerals of all samples were removed by magnetic selection. The purity of quartz grains was checked by IR (830 nm) stimulation to monitor the presence of feldspar. In addition, X-ray diffraction (XRD) was also applied in order to confirm the lack of feldspar, and the results showed that the quartz content was between 98.7% and 100%. Any samples with obvious infrared stimulated luminescence (IRSL) signals were retreated with H_2SiF_6 to avoid D_e underestimated (Lai, 2010). Finally, pure quartz sample of three grain size were washed and cleaned with distilled water, and dried at low temperature. The quartz grains were then mounted on the center part (with a diameter of ~0.5 cm) of stainless steel disks (with a diameter of 1 cm) using silicone oil.

OSL measurement were made using an automated Risø TL/OSL-DA-20 reader equipped with blue diodes (λ=470 ± 5 nm) and IR laser diodes (λ=880 ± 60 nm).

Table 1. *Sample number and its sampling depth as well as environmental radioactivity and OSL dating results of HH-2017.*

Sample ID	Depth (m)	Dating grain size (μm)	K (%)	Th (ppm)	U (ppm)	Water content (%)	No. of aliquots	Dose rate (Gy/ka)	Final D_e (Gy)	OSL age (ka)
HH-2017-01	4.25	4 ~ 11	2.52 ± 0.07	15.70 ± 0.42	2.94 ± 0.11	29 ± 5	11[b]	3.1 ± 0.2	2.6 ± 0.3	0.8 ± 0.1
HH-2017-02	5.17	4 ~ 11	2.71 ± 0.08	15.00 ± 0.40	2.66 ± 0.10	27 ± 5	12[b]	3.3 ± 0.2	1.1 ± 0.1	0.4 ± 0.0
HH-2017-03	6.25	4 ~ 11	2.45 ± 0.07	13.60 ± 0.38	3.32 ± 0.13	30 ± 5	12[b]	3.0 ± 0.2	2.5 ± 0.1	0.8 ± 0.1
HH-2017-04	7.25	4 ~ 11	2.59 ± 0.08	15.60 ± 0.42	2.89 ± 0.11	35 ± 5	12[b]	2.8 ± 0.2	2.7 ± 0.0	1.0 ± 0.1
HH-2017-05	8.28	4 ~ 11	2.23 ± 0.07	14.20 ± 0.38	2.40 ± 0.10	27 ± 5	12[b]	2.8 ± 0.2	2.2 ± 0.1	0.8 ± 0.1
HH-2017-06	10.05	38 ~ 63	1.75 ± 0.06	13.80 ± 0.39	2.38 ± 0.10	35 ± 5	6[a]+11[b]	2.0 ± 0.1	8.0 ± 0.2	3.9 ± 0.2
HH-2017-07	12.56	38 ~ 63	2.03 ± 0.06	11.40 ± 0.32	2.15 ± 0.09	26 ± 5	6[a]+12[b]	2.4 ± 0.2	12.6 ± 0.2	5.2 ± 0.4
HH-2017-08	13.59	38 ~ 63	1.88 ± 0.06	12.30 ± 0.34	2.13 ± 0.09	26 ± 5	6[a]+12[b]	2. 4 ± 0.2	12.0 ± 0.3	5.1 ± 0.4
HH-2017-09	14.24	38 ~ 63	2.07 ± 0.06	14.60 ± 0.39	2.40 ± 0.09	28 ± 5	6[a]+12[b]	2. 6 ± 0.2	12.5 ± 0.2	4.9 ± 0.4
HH-2017-10	15.41	90 ~ 125	1.92 ± 0.06	10.70 ± 0.31	2.11 ± 0.09	30 ± 5	6[a]+12[b]	2.2 ± 0.2	14.0 ± 0.5	6.6 ± 0.5
HH-2017-11	16.53	90 ~ 125	1.65 ± 0.05	8.50 ± 0.26	1.45 ± 0.07	24 ± 5	6[a]+12[b]	1.9 ± 0.1	12.1 ± 0.3	6.3 ± 0.5
HH-2017-12	17.70	90 ~ 125	1.64 ± 0.05	7.90 ± 0.25	1.88 ± 0.08	25 ± 5	6[a]+12[b]	1.9 ± 0.1	11.5 ± 0.2	6.0 ± 0.4
HH-2017-13	18.90	90 ~ 125	1.44 ± 0.05	12.90 ± 0.36	1.97 ± 0.09	22 ± 5	5[a]+12[b]	2.2 ± 0.2	15.3 ± 0.5	7.1 ± 0.5
HH-2017-15	22.34	90 ~ 125	1.50 ± 0.05	10.00 ± 0.29	1.47 ± 0.07	21 ± 5	5[a]+12[b]	2.0 ± 0.1	11.9 ± 0.4	6.1 ± 0.5
HH-2017-17	24.74	90 ~ 125	1.61 ± 0.05	11.00 ± 0.31	1.52 ± 0.07	24 ± 5	6[a]+11[b]	2.0 ± 0.1	13.9 ± 0.8	6.9 ± 0.6
HH-2017-19	27.01	90 ~ 125	2.11 ± 0.06	6.84 ± 0.23	1.12 ± 0.06	27 ± 5	6[a]+12[b]	2.0 ± 0.2	16.0 ± 0.6	8.0 ± 0.7
HH-2017-21	34.11	90 ~ 125	1.69 ± 0.06	6.53 ± 0.22	1.11 ± 0.06	17 ± 5	6[a]+12[b]	2.0 ± 0.2	16.1 ± 0.8	8.2 ± 0.7
HH-2017-22	35.26	90 ~ 125	2.00 ± 0.06	13.50 ± 0.38	3.04 ± 0.12	21 ± 5	6[a]+12[b]	2. 9 ± 0.2	28.0 ± 1.0	10.0 ± 0.8
HH-2017-23	35.95	90 ~ 125	1.90 ± 0.06	12.50 ± 0.35	2.17 ± 0.09	22 ± 5	6[a]+12[b]	2.6 ± 0.2	22.5 ± 0.6	8.9 ± 0.7
HH-2017-25	38.55	90 ~ 125	2.25 ± 0.06	7.74 ± 0.25	1.40 ± 0.07	10 ± 5	6[a]+6[b]	2.8 ± 0.2	21.8 ± 0.9	7.9 ± 0.7

[a] aliquot number used for SAR; [b] aliquot number used for SGC.

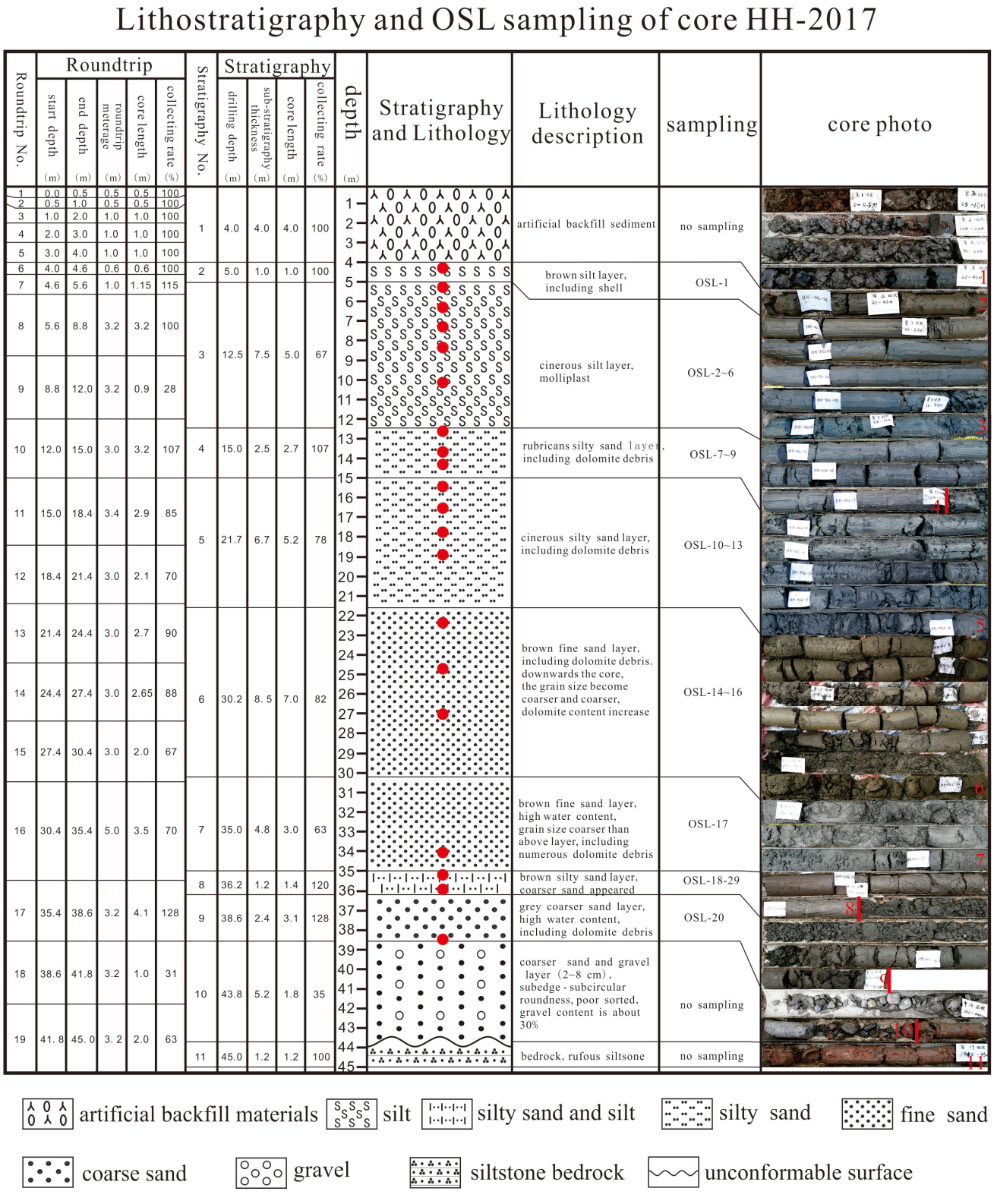

Fig. 2. *Drilling information and profile sketches locating the stratigraphic sampling location for the OSL dating. Before 4.25 m, it is artificial backfill layer while it is gravel layer after 38.55 m; thus, 20 samples totally were collected for OSL dating from 4.25 to 38.55 m.*

The luminescence was stimulated by blue LEDs at 130°C for 40 s, and detected using a 7.5 mm thick U-340 filter (detection window 275–390 nm) in front of the photomultiplier tube. 90% diode power was used. Irradiations were carried out using a $^{90}Sr/^{90}Y$ beta source installed in the Risø reader.

A preheat plateau test and dose recovery test were conducted on sample HH-2017-12 to select a proper preheat temperature. The D_es were tested under different preheat temperatures from 160 to 300°C with a 20°C interval, and the results show a D_e plateau at 240~280°C (**Fig. 3a**). A dose recovery test (Murray and Wintle, 2003) were conducted with different preheat temperatures and the ratios of recovered dose to a given dose (16 Gy) showed the preheat temperature of 240 and 280°C are better (**Fig. 3b**). The stable recycling ratio (**Fig. 3c**) and relative lower thermal transfer ratio (**Fig. 3d**) of 260°C further suggested the preheat temperature of 260°C for 10 s for natural and regenerative doses, and cut-heat was at 220°C for 10 s for test doses for quartz. Signals of the first 0.64 s stimulation were integrated for growth curve construction after background subtraction (last 10 seconds). The concentrations of U, Th and K were measured by neutron activation analysis. The cosmic-ray dose rate was estimated for each sample as a function of depth, altitude and geo-magnetic latitude (Prescott and Hutton, 1994). The dose rates are shown in **Table 1**.

Equivalent dose determination

In the current study, the combination of the Single Aliquot Regeneration (SAR) protocol (Murray and Wintle, 2000) and the Standard Growth Curve (SGC) method (Roberts and Duller, 2004; Lai, 2006; Lai *et al.*, 2007; Yu and Lai, 2012, 2014), named as SAR-SGC method (Lai ad Ou, 2013), was employed for D_e determination. In this method, for each sample, 6–12 aliquots were measured using SAR protocol to get 6–12 growth curves, which were then averaged to construct an SGC for this individual sample, e.g., the SGC of sample HH-2017-10 and HH-2017-23, **Fig. 4a** and **4b**. Then more aliquots were measured to obtain the values of test-dose corrected natural signals only, and each of the values could be matched in the SGC to obtain a D_e. For each sample, the final D_e is the average of the SAR D_es and SGC D_es. The OSL decay curves (**Fig. 4c** and **4d**) decaying to the level of the background within ca. 2 s demonstrate that these signals were mainly from the fast components. Thus, the samples were suitable for OSL dating.

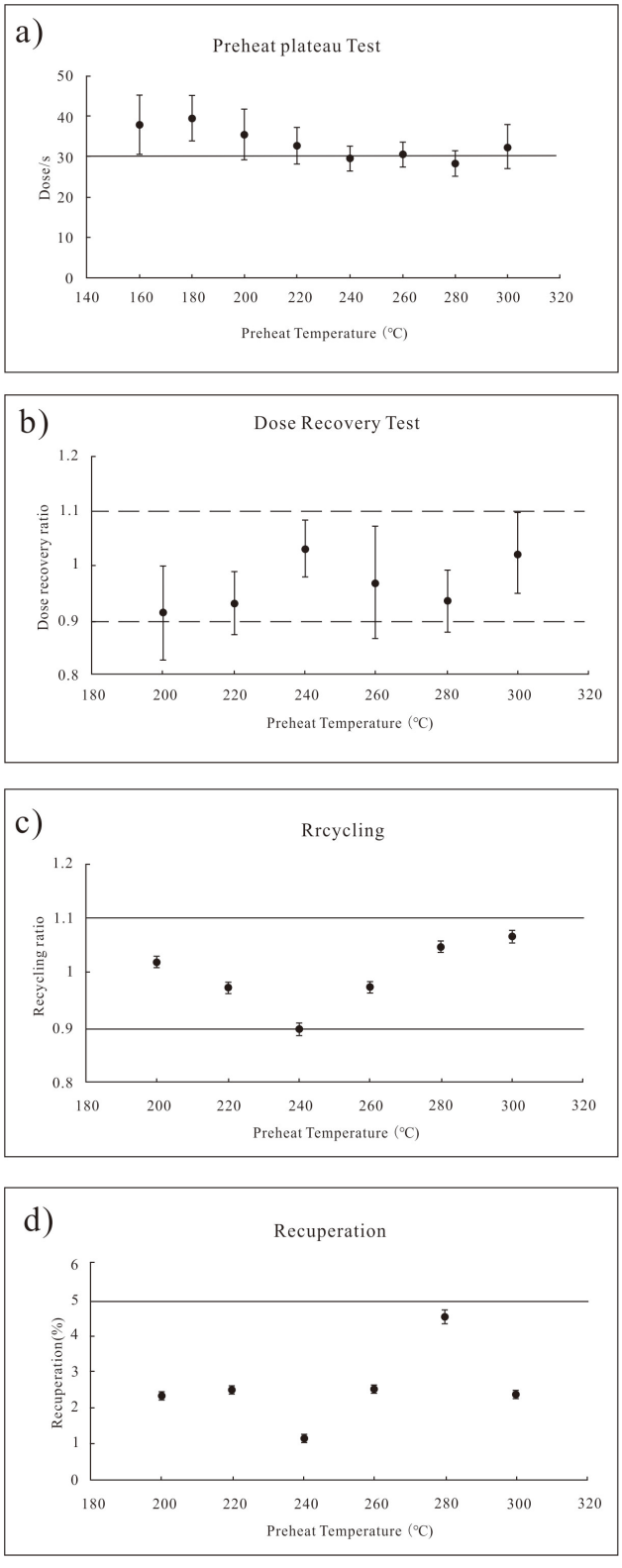

Fig. 3. *Luminescence characteristics of sample HH-2017-12 under different preheat temperature. a) preheat plateau tests; b) dose recovery test; c) recycling ratio; and d) thermo transfer ratio.*

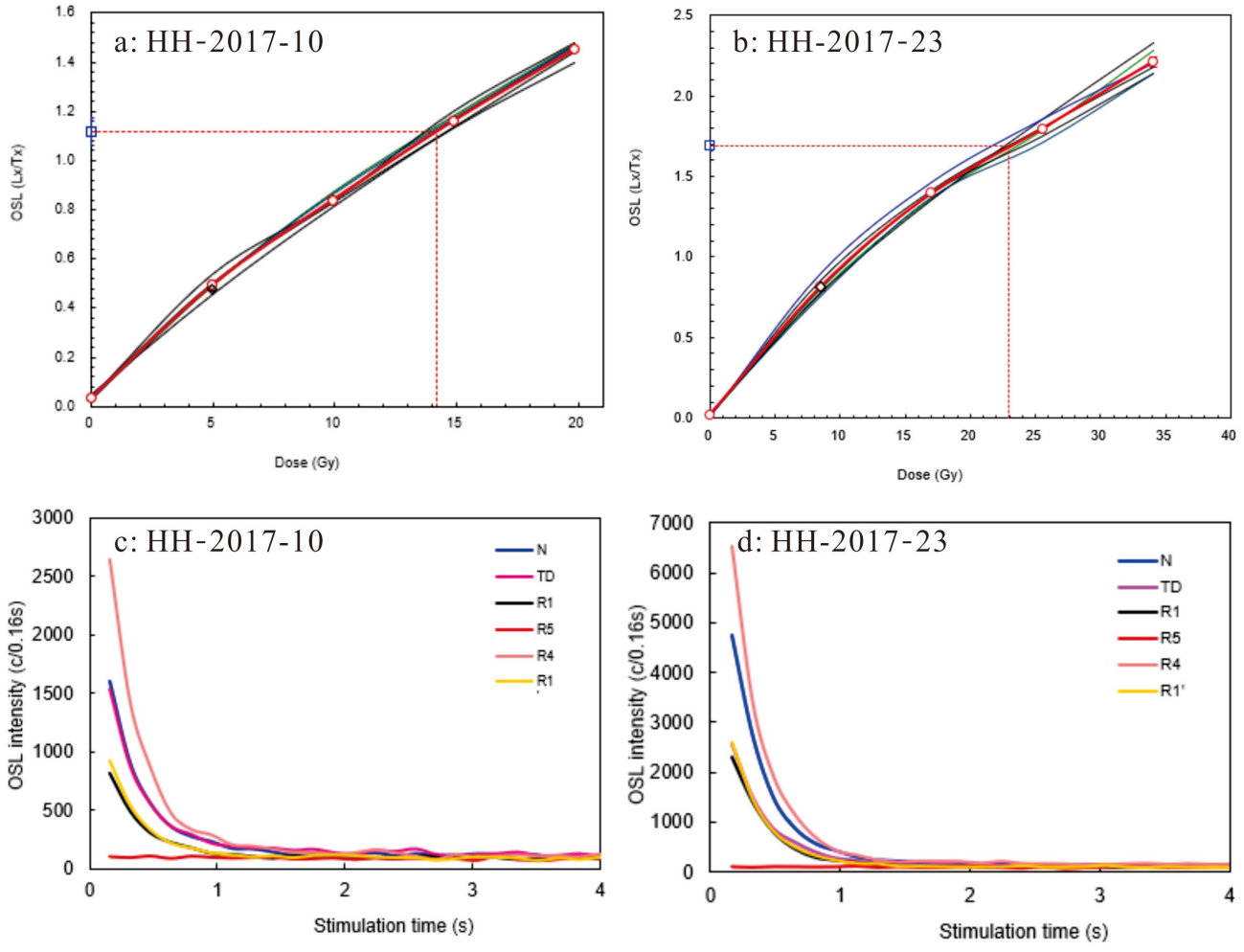

Fig. 4. *Growth and decay curves of sample HH-2017-10 and HH-2017-23.*

4. RESULTS AND DISCUSSIONS

OSL dating results

OSL dating results are presented in **Table 1** and **Fig. 5**. The analytical results show that all these ages range from 0.8 ± 0.1 to 7.9 ± 0.7 ka, and most of them follow the stratigraphic sequence within the normal range of error. Disordered OSL dating may be caused by special transport process of flu-lacustrine sediment, especially of "partly re-erosion and re-deposition" in large river deposystem (Kawakami *et al.*, 2004). The borehole drilled nearby mainstream of the Yangtze River is sensitive to the climate and geo-environment change. The sediments could be of fluvial or lacustrine origin under normal conditions, but also may be derived from extreme climate events, such as occasionally short-term flooding. The reversed age to depth might be caused by the quick deposition process, or ages cannot distinguish the deposition time due to the large error in age calculation. But it's worth noting that the age inversions around 20 cm (~0.8 ka) and 37 cm (~0.4 ka) core depth may be caused by partly exposure of dating materials. This is because that the dose rate of sample HH-2017-02 is equal to its adjunct samples, but the final D_e value is half of its adjunct samples. With the similar sampling and preparation process, we proposed that only partly dating materials exposed to light could reduce the final D_e value, then the younger OSL dating age. However, the results obtained in this study highlight the implication in the application of the OSL dating to flu-lacustrine deposits. The obtained ages also show an increase with depth while the experiments examining luminescence properties are all consistent with the reliable application of the SAR-SGC protocols. In addition, it should be noted that **Fig. 5** also exhibits the sediment of HH-2017 mainly deposited in two periods, the first period is from 7. 9 ± 0.7 to 5.2 ± 0.4 ka, while the second period is between 3.9 ± 0.3 and 0.8 ± 0.2 ka. There is an obvious slow deposition period from 5.2 ± 0.4 to 3.9 ± 0.3 ka.

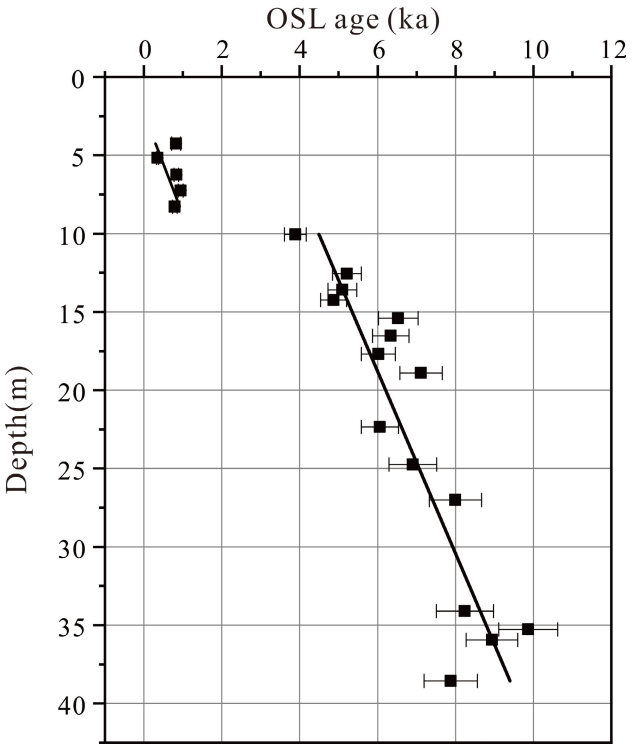

Fig. 5. *Plot of OSL ages against the depth of core HH-2017.*

Widespread lake sediment hiatus of the Wuhan area in middle Holocene

Yao *et al.* (2019) carried out multi AMS ^{14}C dating in various cores in middle and lower reaches of the Yangtze River Basin. Their result combined with previous studies results showed that there was widespread hiatus of sediment during 6~3 ka in lakes from both sides of the middle and lower reaches of the Yangtze River in Holocene (Boyle *et al.*, 1999; Yang *et al.*, 2004; Yao *et al.*, 2006; Gu *et al.*, 2008; Yao *et al.*, 2015). Based on the reconstructed water level data of the Yangtze River and sea level, the authors proposed that during 6~3 ka, water level of the Yangtze River was relatively stable, although sediments were accumulated in lakes, they were easy to be eroded and transported due to relatively high elevation of water-sediment and the impact of Yangtze River, resulting in discontinuity of deposition. One of the possible reasons for lake sediment hiatus during this period is that the inflow of sediment in the upper reaches of the Yangtze River decreases and natural levees are easily destroyed, resulting in the deduction of blocking effect on lakes from both sides of the Yangtze River and making lake sediments easily to be eroded into the river (Yao *et al.*, 2019). As located at middle Yangtze River reaches, our OSL dating results of HH-2017 are partly corresponding with the results of previous studies, which demonstrated that our OSL dating results was reliable rather than problematic in experiment and age calculation.

Relationship between lithology change and climate change

Changes in sedimentary lithology and apparent accumulation rate indicate the depositional model change. In millennial-scale, only a minor change showed in tectonic activity and terrain slope, which hardly resulted in such a quickly deposition rate and sedimentary environment change in Wuhan area. Thus, we propose that Holocene climate change and increasing human activity contributes to these phenomena.

At about 21.6 m of HH-2017, the sediment grain size changes from fine sand to silty sand. OSL dating results show that the sedimentary layer deposits between 6.4 and 5.5 ka, which is closely related to Asian summer monsoon weakened period recorded by stalagmite of Heshang cave, Hubei province and Dongge cave, Guizhou province, China from 6.2 to 5.4 ka. (Cosford *et al.*, 2008; Li *et al.*, 2014; Wang *et al.*, 2014; Yun *et al.*, 2015). The paleo-hydrological conditions since 13 ka. in this region based on the synthesis of 4 proxies extracted from the Dajiuhu peatland and above two cave stalagmites show that period of 6.4–5.5 ka is a long-term drier period (Xie *et al.*, 2013, 2015; Zhang *et al.*, 2016). However, it is notable that in the middle Yangtze River region, most drier periods occurred at the warm conditions, different from the cold-drought association in North China. Thus, the climate variation changes the rainfall capacity and surface flow, then the sediment grain size. In addition, high resolution paleoclimate records from pollen, peat, ice core and ocean sediments also indicate that there is a significant climate change during 6~5 ka, which is also recorded in the HH-2017 lithology change (Qin *et al.*, 2012; Huang *et al.*, 2012; Li *et al.*, 2014; Zhang *et al.*, 2017).

During 5.2~3.9 ka, there is a slow sediment accumulation in HH-2017. Various stalagmite record in the middle Yangtze River region also indicates that the region is drier at about 4.2 ka (Xie *et al.*, 2015). Rainfall reduction makes both surface flow erosion capacity and river carrying capacity decreased, then less sediment contribution and low depositing rate in this region. In addition, historical documentation also indicates that there is great climate variability between approximately 5~4 ka all over the world (Mayewski *et al.*, 2004; Daley *et al.*, 2010; Bringué and Rochon, 2012; Litt *et al.*, 2012; Zhu *et al.*, 2017; Huang *et al.*, 2018; Wang *et al.*, 2018; Zhang *et al.*, 2018).

Relationship between lithology change and enhanced human activity

Since 1 ka, rapidly increasing population in middle Yangtze River needs more land to produce food. During the Song dynasty (960–1279 a A.D.) and Ming dynasty (1368–1644 a A.D.), the perennial heavy incursions of the northern nomads resulting in the economic centre moved from north China to middle Yangtze River, and

then Wuhan area became the economic centre of the middle reaches of the Yangtze River with its preponderant amphibious transportation (Wang, 1990; Shi, 1991). In addition, Zhang and Zhang (2010) reported that the crop loss was caused by the weather cooling in north China also contributed to the migration of population and economic centre. Agriculture and deforestation are expected to increase the sediment yield, but reservoirs can trap much of this sediment before it reaches the Yangtze River. Consequently, enhanced human activity of reclaiming farmland from lakes make lots of artificial lakes in this area (Zhou and Mi, 1998; Sun *et al.*, 2016). Many studies have recognised that human activities can significantly change the erosion-deposition patterns and rates (Bayon *et al.*, 2012; Hu *et al.*, 2013; He *et al.*, 2014; Reusser *et al.*, 2015; Wan *et al.*, 2015). Thus, lacustrine sediment widely developed in Wuhan area after 1 ka.

5. CONCLUSIONS

Luminescence characteristics, including preheat temperature, lab dose recovery, OSL decay and growth curve, and ages distribution show that the OSL signal of flu-lacustrine sediments from core HH-2017 was reset before burial and that OSL dating could have considerable potential for improving the chronology of Holocene flu-lacustrine sediments in Wuhan area.

The good agreement between the OSL ages, stratigraphic sequence, and climate background suggests that OSL dating method could establish significant chronology framework for fluvial sediment in large river drainage, which lack of suitable materials for ^{14}C dating. In addition, relatively high resolution OSL ages of HH-2017 would provide a powerful chronology for reconstructing paleoclimate change and paleo-environment evolution in the Wuhan area, China.

ACKNOWLEDGEMENT

This work was supported by the National Science Foundation of China (No. 41871019 and 41672355).

REFERENCES

Ashley GM, Ndiema EK, Spencer JQG, Harris JWK and Kiura PW, 2011. Paleoenvironmental context of archaeological sites, implications for subsistence strategies under Holocene climate change, northern Kenya. *Geoarchaeology an International Journal* 26(6): 809–837, DOI 10.1002/gea.20374.

Bayon G, Dennielou B, Etoubleau J, Ponzevera E, Toucanne S and Bermell S, 2012. Intensifying weathering and land use in iron age Central Africa. *Science* 335(6073): 1219–1222, DOI 10.1126/science.1215400.

Berger G and Doran P, 2001. Luminescence-dating zeroing tests in Lake Hoare, Taylor Valley, Antarctica. *Journal of Paleolimnology* 25(4): 519–529, DOI 10.1023/A:1011144502713.

Boyle JF, Rose NL, Bennion H, Yang H and Appleby PG, 1999. Environmental Impacts in the Jianghan Plain: Evidence from Lake Sediments. *Water Air and Soil Pollution* 112(1): 21–40, DOI 10.1023/A:1005040713678.

Briner JP, Mckay NP, Axford Y, Bennike O, Bradley RS, Vernal AD, Fisher D, Francus P, Frechette B, Gajewski K, Jennings A, Kaufman DS, Miller G, Rouston C and Wagner B, 2016. Holocene climate change in Arctic Canada and Greenland. *Quaternary Science Reviews* 147: 340–364, DOI 10.1016/j.quascirev.2016.02.010.

Bringué M and Rochon A, 2012. Late Holocene paleoceanography and climate variability over the Mackenzie Slope (Beaufort Sea, Canadian Arctic). *Marine Geology* 291–294(4): 83–96, DOI 10.1016/j.margeo.2011.11.004.

Cosford J, Qing H, Eglington B, Mattey D, Yuan D, Zhang M and Cheng H, 2008. East Asian monsoon variability since the Mid-Holocene recorded in a high-resolution, absolute-dated aragonite speleothem from eastern China. *Earth and Planetary Science Letters* 275(3–4): 296–307, DOI 10.1016/j.epsl.2008.08.018.

Cupper ML, 2008. Luminescence and radiocarbon chronologies of playa sedimentation in the Murray Basin, southeastern Australia. *Quaternary Science Reviews* 25(19): 2594–2607, DOI 10.1016/j.quascirev.2005.09.011.

Daley TJ, Barber KE, Street-Perrott FA, Marshall J, Crowley S and Fisher L, 2010. Holocene climate variability revealed by oxygen isotope analysis of Sphagnum, cellulose from Walton Moss, northern England. *Quaternary Science Reviews* 29(13): 1590–1601, DOI 10.1016/j.quascirev.2009.09.017.

English P, Spooner NA, Chappell J, Questiaux DG and Hill NG, 2001. Lake Lewis basin, central Australia: environmental evolution and OSL chronology. *Quaternary International* 83(01): 81–101, DOI 10.1016/S1040-6182(01)00032-5.

Fan QS, Lai ZP, Long H, Sun YJ and Liu XG, 2010. OSL chronology for lacustrine sediments recording high stands of Gahai Lake in Qaidam Basin, northeastern Qinghai–Tibetan Plateau. *Quaternary Geochronology* 5(2): 223–227, DOI 10.1016/j.quageo.2009.02.012.

Gu YS, Qiu HO, Xie SC, Huang JH and Zhou XG, 2008. Lake sediment records for eutrophication history in response to human activity during recent century in the Liangzi Lake, Hubei Province. *Earth Science-Journal of China University of Geosciences* 33(5): 679–686 (in Chinese with English abstract).

Guo L, Xiong S, Ding ZL, Jin GY, Wu JB and Ye W, 2018. Role of the mid-Holocene environmental transition in the decline of late Neolithic cultures in the deserts of NE China. *Quaternary Science Reviews* 190: 98–113, DOI 10.1016/j.quascirev.2018.04.017.

Harning DJ, Thordarson T, Geirsdóttir A, Zalzal K and Miller GH, 2018. Provenance, stratigraphy and chronology of Holocene tephra from Vestfireir, Iceland. *Quaternary Geochronology* 46: 59–76, DOI 10.1016/j.quageo.2018.03.007.

He MY, Zheng HB, Bookhagen B and Clift PD, 2014. Controls on erosion intensity in the Yangtze River basin tracked by U-Pb detrital zircon dating. *Earth-Science Reviews* 136: 121–140, DOI 10.1016/j.earscirev.2014.05.014.

Hu DK, Clift PD, Böning P, Hannigan R, Hillier S, Blusztajn J, Wan SM and Fuller DQ, 2013. Holocene evolution in weathering and erosion patterns in the Pearl River delta. *Geochemistry, Geophysics, Geosystems* 14(7): 2349–2368, DOI 10.1002/ggge.20166.

Hu G, Yi CL, Zhang JF, Cao GR, Pan BL, Liu JH, Tao J, Yi SW, Li DH and Huang JW, 2017. Chronology of a lacustrine core from Lake Linggo Co using a combination of OSL, 14C and 210Pb dating: implications for the dating of lacustrine sediments from the Tibetan Plateau. *Boreas* 47(2): 656–670, DOI 10.1111/bor.12291.

Huang XY, Meyers PA, Yu JX, Wang XX, Huang JH, Jin F Gu YS and Xie SC, 2012. Moisture conditions during the Younger Dryas and the early Holocene in the middle reaches of the Yangtze River, central China. *Holocene* 22(12): 1473–1479, DOI 10.1177/0959683612450202.

Huang XY, Pancost RD, Xue JT, Gu YS, Evershed R and Xie SC, 2018. Response of carbon cycle to drier conditions in the mid-Holocene in central China. *Nature Communications* 9(1): 1369, DOI 10.1038/s41467-018-03804-w.

Ideker CJ, Finley JB, Rittenour M and Nelson MS, 2017. Single-grain optically stimulated luminescence dating of quartz temper from prehistoric Intermountain Ware ceramics, northwestern Wyoming,

USA. *Quaternary Geochronology* 42: 45–55, DOI 10.1016/j.quageo.2017.07.004.

Kawakami I, Matsuo M, Kato M and Fukusawa H, 2004. Chronology and sedimentation process of varved lacustrine sediment in Lake Fukami, central Japan. *Quaternary International* 123: 27–34, DOI 10.1016/j.quaint.2004.02.005.

Lai ZP and Ou XJ, 2013. Basic procedures of optically stimulated luminescence (OSL) dating. *Progress in Geography* 32(5): 683–693 (in Chinese with English abstract).

Lai ZP, 2006. Testing the use of an OSL standardised growth curve (SGC) for De determination on quartz from the Chinese Loess Plateau. *Radiation Measurements* 41(1): 9–16, DOI 10.1016/j.radmeas.2005.06.031.

Lai ZP, 2010. Chronology and the upper dating limit for loess samples from Luochuan section in the Chinese Loess Plateau using quartz OSL SAR protocol. *Journal of Asian Earth Sciences* 37: 176–185, DOI 10.1016/j.jseaes.2009.08.003.

Lai ZP, Brückner H, Zöller L and Fülling A, 2007. Existence of a common growth curve for silt-sized quartz OSL of Loess from different continents. *Radiation Measurements* 42(9): 1432–1440, DOI 10.1016/j.radmeas.2007.08.006.

Lehmann B, Valla PG, King GE, King GE and Herman F, 2017. Investigation of OSL surface exposure dating to reconstruct post-LIA glacier fluctuation in the French Alps (Mer de Glace, Mont Blanc massif). *Quaternary Geochronology* 44: 63–74, DOI 10.1016/j.quageo.2017.12.002.

Li F, Zhu C, Wu L, Sun W, Liu H, Chyi SJ, Kuang CL, Zhu GY and Wang XC, 2014. Environmental humidity changes inferred from multi-indicators in the Jianghan Plain, Central China during the last 12,700 years. *Quaternary International* 349(349): 68–78, DOI 10.1016/j.quaint.2013.09.040.

Litt T, Ohlwein C, Neumann F, Hense A and Stein M, 2012. Holocene climate variability in the Levant from the Dead Sea pollen record. *Quaternary Science Reviews* 49(3): 95–105, DOI 10.1016/j.quascirev.2012.06.012.

Liu XQ, Dong HL, Yang XD, Herzschuh U, Zhang EL, Stuut JB and Wang YB, 2009. Late Holocene forcing of the Asian winter and summer monsoon as evidenced by proxy records from the northern Qinghai–Tibetan Plateau. *Earth and Planetary Science Letters* 280(1–4): 0–284, DOI 10.1016/j.epsl.2009.01.041.

Long H, Lai ZP, Wang NA and Zhang JR, 2011. A combined luminescence and radiocarbon dating study of Holocene lacustrine sediments from arid northern China. *Quaternary Geochronology* 6(1): 1–9, DOI 10.1016/j.quageo.2010.06.001.

Lu YC, Wang XL and Wintle AG, 2007. A new OSL chronology for dust accumulation in the last 130,000 yr for the Chinese Loess Plateau. *Quaternary Research* 67(1): 152–160, DOI 10.1016/j.yqres.2006.08.003.

Madsen DB, Ma HZ, David R, Brantingham PJ and Forman SL, 2008. Age constraints on the late Quaternary evolution of Qinghai Lake, Tibetan Plateau. *Quaternary Research* 69(2): 316–325, DOI 10.1016/j.yqres.2007.10.013.

Marks L, Salem A, Welc F, Nitycoruk J, Chen ZY, Blaauw M, Zalat A, Majecka A, Szymanek M, Chodyka M, Tolczko-Pasek A, Sun QL, Zhao XS and Jiang J, 2017. Holocene lake sediments from the Faiyum Oasis in Egypt: a record of environmental and climate change. *Boreas* 47(1): 62–79, DOI 10.1111/bor.12251.

May JH, Marx SK, Reynolds W, Clark-Balzan L, Jacobsen GE and Preusser F, 2018. Establishing a chronological framework for a late quaternary seasonal swamp in the Australian 'Top End'. *Quaternary Geochronology* 47: 81–92, DOI 10.1016/j.quageo.2018.05.010.

Mayewski PA, Rohling EE, Curt SJ, Karlen W. Maasch K, Meeker LD, Meyerson EA, Gasse F, Kreveld SV, Holmgren K, Lee-Thorp J, Rosqvist G, Rack F, Staubwasser M, Schneider RR and Steig EJ, 2004. Holocene Climate Variability. *Quaternary Research* 62(3): 243–255, DOI 10.1016/j.yqres.2004.07.001.

Murray AS and Wintle AG, 2000. Luminescence dating of quartz using an improved single-aliquot regenerative-dose protocol. *Radiation Measurements* 32(1): 57–73, DOI 10.1016/s1350-4487(99)00253-x.

Murray AS and Wintle AG, 2003. The single aliquot regenerative dose protocol: potential for improvements in reliability. *Radiation Measurements* 37(4–5): 377–381, DOI 10.1016/s1350-4487(03)00053-2.

Olley JM, Pietsch T and Roberts RG, 2004. Optical dating of Holocene sediments from a variety of geomorphic settings using single grains of quartz. *Geomorphology* 60(3–4): 0–358, DOI 10.1016/j.geomorph.2003.09.020.

Ozcelik M, 2016. Optically stimulated luminescence (OSL) dating of quartz grains within the sand dykes cutting the lacustrine deposits in the Burdur area (SW Turkey) and its tectonic interpretation. Arabian *Journal of Geosciences* 9(1): 21, DOI 10.1007/s12517-015-2034-x.

Prescott JR and Hutton JT, 1994. Cosmic ray contribution to dose rates for lumines-cence and ESR dating: large depths and long-term time variations. *Radiation Measurements* 23(2–3): 497–500, DOI 10.1016/1350-4487(94)90086-8.

Prokopenko AA, Khursevich GK, Bezrukova EV, Kuzmin MI, Boes X, Williams DF, Fedenya SA, Kulagina NV, Letunova PP and Abzaeva AA, 2007. Paleoenvironmental proxy records from Lake Hovsgol, Mongolia, and a synthesis of Holocene climate change in the Lake Baikal watershed. *Quaternary Research* 68(1): 2–17, DOI 10.1016/j.yqres.2007.03.008.

Qin Y, Payne RJ, Gu YS, Huang XY and Wang HM, 2012. Ecology of testate amoebae in Dajiuhu peatland of Shennongjia Mountains, China, in relation to hydrology. *Frontiers of Earth Science* 6(1): 57–65, DOI 10.1007/s11707-012-0307-1.

Queiroz-Alves E, Macario K, Ascough P and Ramsey CB, 2018. The worldwide marine radiocarbon reservoir effect: Definitions, mechanisms and prospects. *Reviews of Geophysics* 56(1): 278–305, DOI 10.1002/2017RG000588.

Reusser L, Bierman P and Rood D, 2015. Quantifying human impacts on rates of erosion and sediment transport at a landscape scale. *Geology* 43(2): 171–174, DOI 10.1130/G36272.1.

Roberts HM and Duller GAT, 2004. Standardised growth curves for optical dating of sediment using multiple-grain aliquots. *Radiation Measurements* 38(2): 241–252, DOI 10.1016/j.radmeas.2003.10.001.

Shen HY, Yu LP, Zhang HM, Zhao M and Lai ZP, 2015. OSL and radiocarbon dating of flood deposits and its paleoclimatic and archaeological implications in the Yihe River Basin, East China. *Quaternary Geochronology* 30: S1871101415000540, DOI 10.1016/j.quageo.2015.03.005.

Shi HJ, 1991. The geographical foundation of economic center moving southward in Tang dynasty and Song dynasty. *Journal of Nanjing Normal University (Social Science Edition)* 3: 35–42 (in Chinese).

Sun XL, Li CA, Kuiper KF, Zhang ZJ, Gao JH and Wijbrans JR, 2016. Human impact on erosion patterns and sediment transport in the Yangtze River. *Global and Planetary Change* 143: 88–99, DOI 10.1016/j.gloplacha.2016.06.004.

Wallinga J, 2010. Optically stimulated luminescence dating of fluvial deposits: a review. *Boreas* 31(4): 303–322, DOI 10.1111/j.1502-3885.2002.tb01076.x.

Wan SM, Toucanne S, Clift PD, Zhao DB, Bayon G, Yu ZJ, Cai GQ, Yin XB, Révillon S and Wang DW, 2015. Human impact overwhelms long-term climate control of weathering and erosion in southwest China. *Geology* 43(5): 439–442, DOI 10.1130/G36570.1.

Wang CF, Bendleb JA., Zhang HB, Yang Y, Liu D, Huang JH, Cui JW and Xie SC, 2018. Holocene temperature and hydrological changes reconstructed by bacterial 3-hydroxy fatty acids in a stalagmite from central China. *Quaternary Science Reviews* 192: 97–105, DOI 10.1016/j.quascirev.2018.05.030.

Wang K, Zheng HB, Tada R, Irino T, Zheng Y, Saito K and Karasuda A, 2014. Millennial-scale East Asian Summer Monsoon variability recorded in grain size and provenance of mud belt sediments on the inner shelf of the East China Sea during mid-to late Holocene. *Quaternary International* 349: 79–89, DOI 10.1016/j.quaint.2014.09.014.

Wang PX, Clemens S, Beaufort L, Braconnot P, Ganssen G, Jian ZJ, Kershaw P and Sarnthein M, 2017. Evolution and variability of the

Asian monsoon system: state of the art and outstanding issues. *Quaternary Science Reviews* 24(5): 595–629, DOI 10.1016/j.quascirev.2004.10.002.

Wang SM, 1990. On the southward movement of the economic center of the Song dynasty. J*ournal of Qinghai Normal University (Philosophy and Social Sciences Edition)* 04: 45–50 (in Chinese). DOI 10.16229/j.cnki.issn1000-5102.1990.04.009.

Wang Y, Ji S, Wu J, Liu XQ, Zhang EL and Liu EF, 2007. Hard-water effect correction of lacustrine sediment ages using the relationship between ~ (14)C levels in lake waters and in the atomosphere: the case of Lake Qinghai. *Journal of Lake Science* 19(5): 504–508, DOI 10.18307/2007.0502.

Xie SC, Evershed RP, Huang XY, Zhu ZM, Pancost RD, Meyers PA, Gong LF, Hu CY, Zhang SH, Gu YS and Zhu, JY, 2013. Concordant monsoon-driven postglacial hydrological changes in peat and stalagmite records and their impacts on prehistoric cultures in central China. *Geology* 41(8): 827–830, DOI 10.1130/g34318.1.

Xie SC, Hu C, Gu Y and Huang XY, 2015. Paleohydrological Variation since 13ka BP in Middle Yangtze Region. *Earth Science* 40(2): 198–205, DOI 10.3799/dqkx.2015.015.

Xu L, Shi YJ, Chen XD and Wan CZ, 2018. Kinetic analysis of hydrocarbon generation based on saline lacustrine source rock and kerogen samples in the western Qaidam Basin, China. *Carbonates and Evaporites* 1–3: 1–9, DOI 10.1007/s13146-018-0462-x.

Yang H, Yi CL, Xing YP and Yang T, 2004. A comparative study on recent sedimentation rates in Lake Donghu, Wuhan with ^{210}Pb and ^{137}Cs dating techniques. *Journal of Central China Normal University (Natural Science)* 38(1): 109–113 (in Chinese with English abstract).

Yao SC, Li CH, Ling CH, Zhang K, Zhou ZZ, Liu JL, Tao YQ, Cheng LJ and Bin X, 2019. About 3000 years of lake sediment hiatus due to relatively stable water level of the Yangtze River in the middle Holocene. *Quaternary Sciences* 39(5): 1148–1158, DOI 10.11928/j.issn.1001-7410.2019.05.07.

Yao SC, Xue B, Li SJ, Liu JF and Xia WL, 2006. Sedimentation rates in Honghu, Chaohu and Taihu lakes in the middle and lower reaches of the Yangtze River. *Resources and environment in the Yangtze Basin* 15(5): 569–573 (in Chinese with English abstract).

Yao Y, Yang H, Liu WG, Li XZ and Chen YW, 2015. Hydrological changes of the past 1400 years recorded in δD of sedimentary n-alkanes from Poyang Lake, Southeastern China. *The Holocene* 25(7): 1068–1075, DOI 10.1177/0959683615576231.

Yu LP and Lai ZP, 2012. OSL chronology and palaeoclimatic implications of aeolian sediments in the Qaidam Basin of the northeastern Qinghai-Tibetan Plateau. *Palaeogeography, Palaeoclimatology, Palaeoecology* 337–338: 120–129, DOI 10.1016/j.palaeo.2012.04.004.

Yu LP and Lai ZP, 2014. Holocene climate change inferred from stratigraphy and OSL chronology of aeolian sediments in the Qaidam Basin, northeastern Qinghai-Tibetan Plateau. *Quaternary Research* 81(03): 488–499, DOI 10.1016/j.yqres.2013.09.006.

Yun Y, Xiang X, Wang HM, Man BY, Gong LF, Liu QY, Dong Q and Wang RC, 2015. Five-Year Monitoring of Bacterial Communities in Dripping Water from the Heshang Cave in Central China: Implication for Paleoclimate Reconstruction and Ecological Functions. *Geomicrobiology Journal* 33(7): 1–11, DOI 10.1080/01490451.2015.1062062.

Zhang HB, Griffiths ML, Chiang JCH, Kong WW, Wu ST, Atwood A, Huang JH, Ning YF and Xie SC, 2018. East Asian hydroclimate modulated by the position of the westerlies during Termination I. *Science* 362(6414): 580–583, DOI 10.1126/science. aat9393.

Zhang WC, Yan H, Cheng P and Lu FY, 2016. Peatland development and climate changes in the Dajiuhu basin, central China, over the last 14,100 years. *Quaternary International* 425: 273–281, DOI 10.1016/j.quaint.2016.06.039.

Zhang WC, Yan H, Dodson J, Cheng P, Liu CC, Li JY, Lu FY, Zhou WJ and An ZS, 2017. The 9.2 ka event in Asian summer monsoon area: the strongest millennial scale collapse of the monsoon during the Holocene. *Climate Dynamics* 1–16, DOI 10.1007/s00382-017-3770-2.

Zhang ZJ, Tyrrell S, Li CA, Daly S, Sun XL and Li QW, 2015. Pb isotope compositions of detrital K-feldspar grains in the upper-middle Yangtze River system: Implications for sediment provenance and drainage evolution. *Geochemistry Geophysics Geosystems* 15(7): 2765–2779, DOI 10.1002/2014GC005391.

Zhao QY, Thomsen KJ, Murray AS, Wei MJ, Pan BL, Song B, Zhou R, Chen SZ, Zhao XH and Chen HY, 2015. Testing the use of OSL from quartz grains for dating debris flows in Miyun, northeast Beijing, China. *Quaternary Geochronology* 30: 320–327, DOI 10.1016/j.quageo.2015.03.007.

Zhou XH and Mi H, 1998. Climate and crop production in China during the Ming dynasty and Qing dynasty. *Journal of Chinese Social and Economic History* 04: 59–64 (in Chinese). DOI 10.13469/j.cnki.zgshjjsyj.1998.04.009.

Zhou WJ, Xie SC, Meyers PA and Zheng YH, 2005. Reconstruction of late glacial and Holocene climate evolution in southern China from geolipids and pollen in the Dingnan peat sequence. *Organic Geochemistry* 36(9): 1272–1284, DOI 10.1016/j.orggeochem.2005.04.005.

Zhu ZM, Feinberg JM, Xie SC, Bourne-Worster MD, Huang CJ, Hu CY and Cheng H, 2017. Holocene ENSO-related cyclic storms recorded by magnetic minerals in speleothems of central China. *Proceedings of The National Academy of Sciences of the United States of America* 114(5): 852–857, DOI 10.1073/pnas.1610930114.

Zhang YX and Zhang LZ, 2010. The influence of climate change on the southward shift of economic center in Song dynasty. *Henan Social Sciences* 18(3): 117–119 (in Chinese).